

Measurement of Leakage and Identification of Structural Force Coefficients in a Hybrid Brush Seal - Extended Abstract

Luis San Andrés
Mast-Childs Professor
Fellow ASME
Lsanandres@mengr.tamu.edu

José Baker
jbakerv@tamu.edu
Adolfo Delgado
adelgam@tamu.edu

Graduate Research Assistants

Mechanical Engineering Department., Texas A&M University,
College Station, TX 77843, U.S.A.

INTRODUCTION

Current trends in turbomachinery lead to higher pressure differentials, operating temperatures, and rotational speeds. Such operating conditions demand effective control of interface clearance to reduce leakage, and consequently, to improve power delivery. Incorporating state-of-the-art sealing components in turbomachinery reduces leakage and power losses with savings in fuel consumption, operation and maintenance costs, and increases engine reliability.

Brush seals improve power and efficiency in turbomachinery by overcoming the limitations associated to labyrinth seals [1,2,3]. Experiments and field tests demonstrate that brush seals can considerably reduce parasitic leakage [4,5,6]; while promoting rotordynamic stability and reducing excessive engine vibrations [3,7]. Commercially available brush seals consist of packed metallic bristles clamped between a front plate on the upstream (high pressure region) and a backing plate on the downstream (low pressure region). Bristles are slanted at an angle (i.e., lay angle) in the direction of rotor spinning. The bristles bend rather than buckle during transient radial excursions of the rotor.

Currently, the primary limitation of conventional brush seals is their inability to withstand high pressure differentials, excessive bristle wear [5], and localized heat generation during shaft rotation [8]. All of these factors can damage the brush seal permanently and increase its leakage. In addition, conventional brush seals cannot accommodate shaft rotation in both directions, an issue of importance in some aircraft gas turbines.

Justak [9] introduced the 1st generation shoed-brush seal (SBS). This improved brush seal design accommodates shaft rotation in both directions at the same time it eliminates bristle tip wear, pad/rotor contact and thermal distortions by means of a hydrodynamic gas film lifting the pads as the rotor spins. Delgado, et al., [10] present a comprehensive analysis for predicting the rotordynamic force coefficients in a SBS. This analysis is followed by Delgado and San Andrés [11] experiments to extract structural stiffness and damping characteristics from a shoed-brush seal by using single frequency shaker load tests.

Justak [12] later introduced the hybrid brush seal (HBS), a 2nd generation shoed-brush seal, shown in Figure 3. In a HBS, the arcuate pads connect to the seal casing through EDM-webs. The novel construction eliminates reliability issues

associated with the spot-welded connections originally used. More importantly, the thin beam connections (webs) provide a high axial stiffness while maintaining a low radial stiffness; thus reducing pad and rotor wear and secondary flow (leakage) by eliminating pad pitching motions caused by the large pressure differential imposed across the seal. Once the HBS is pressurized, the pad design allows for a hydrostatic lift-off effect, prior to shaft rotation. This effect is further enhanced by the hydrodynamic action generated by the rotation of the shaft.

Justak and Crudgington [13] evaluate the performance and design of a HBS under static (no-rotation) and with shaft rotation conditions (maximum operating speed 15,000 rpm). The seal was tested in both ambient temperature and high temperature test rigs, at pressure differentials ranging from 0 to 300 kPa, to simulate engine conditions.

This paper shows measurements of HBS leakage and structural force coefficients for increasing pressure differentials obtained at room temperature.



Figure 1 Close-up view of hybrid brush seal (HBS) [11]

TEST RIG AND HYBRID BRUSH SEAL (HBS) DESCRIPTION

Figure 2 depicts a cut view of the non-rotating HBS test rig, consisting of an aluminum disk (167.1 mm in diameter and 25.4 mm in length) mounted on a long and slender steel shaft located inside a cylindrical steel vessel. One end of the shaft is affixed to the bottom of the vessel via two rolling elements bearings. The test brush seal (166.4 mm in diameter at the pads circumference) is secured atop the vessel with a retainer ring. The seal assembly nominal radial interference fit

with the disk is 0.38 mm (0.015 in). The air supply line is instrumented with a pressure gauge, a turbine flowmeter, a static pressure transducer, and thermocouples. The test HBS is 166.4 mm in diameter and the pads width is 8.53 mm.

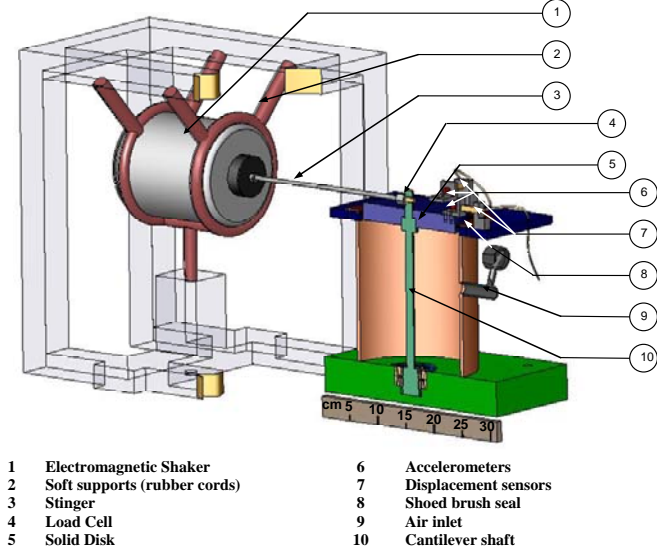


Figure 2 Cut view of non-rotating HBS test rig [11]

LEAKAGE MEASUREMENTS

Leakage in the HBS is measured for increasing supply to discharge pressure ratios, $P_r = P_s / P_d$, (P_s up to 307 kPa) at ambient temperature ($\sim 25^\circ\text{C}$), under static conditions (no shaft rotation). The discharge pressure P_d is ambient (101 kPa). Figure 3 depicts the measured mass flow rate versus pressure ratio ($P_r = P_s / P_d$) under static conditions (i.e. without shaft rotation) for the hybrid brush seal (HBS) and a 1st generation shoed-brush seal (SBS) tested at identical feed pressure conditions by Delgado and San Andrés [11]. The HBS shows a better sealing performance over its predecessor, reducing overall leakage by about 36% over the test pressure range.

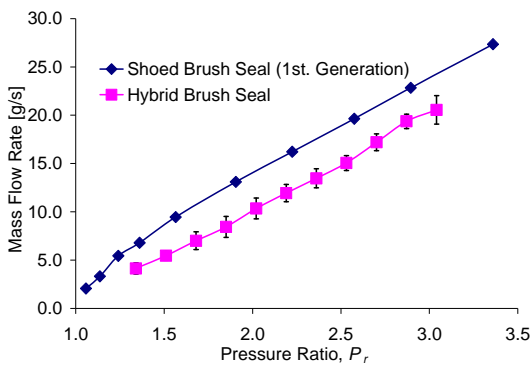


Figure 3 Test flow rates for 1st generation SBS and HBS versus supply to discharge pressure ratio under static conditions (no shaft rotation) [11]

EXPERIMENTAL PROCEDURE AND RESULTS FOR IDENTIFIED STRUCTURAL FORCE COEFFICIENTS

Dynamic load tests were performed in a controlled motion test rig (no rotation) at room temperature (23°C) to characterize the dynamic structural behavior of a HBS under

increasing pressure differentials. The physical model, initially introduced by Delgado and San Andrés [11], estimates the structural stiffness and energy dissipation mechanism of a HBS subjected to a constant unidirectional external excitation force. The system motions are confined to frequencies around its fundamental elastic mode; thus allowing the simplification of the test system to a 1-DOF system. Additionally, the dynamic response shows that the cross-couplings effects, i.e., motions in the orthogonal direction to the excitation force, are negligible (at least one order of magnitude smaller) for the test excitation frequency range and supply pressure conditions. The dynamic load tests consist in exciting the test seal with loads of single-frequency, 20 to 110 Hz, and of three amplitudes (55N, 63N, and 66N). The load magnitudes, as well as the supply pressure, are maintained constant throughout the test frequency range. The tests are conducted for three absolute supply pressures ($P_s=169, 238$ and 307 kPa).

The dynamic response of the HBS involves relative motions of the seal components and bending of the bristles and the slender EDM beams supporting the pads. Thus, the energy dissipation of the test seal is modeled in terms of dry friction coefficient (μ) and a loss factor coefficient (γ) as presented in Ref. [11].

Table 1 list the stiffness, mass and energy dissipation coefficients obtained from the parameter identification procedure for the HBS. The results show that the direct stiffness increases with increasing supply pressure ($\sim 35\%$ for pressure ratios: 1.0 to 3.0).

Table 1 Identified hybrid brush seal (HBS) parameters from dynamic load tests (Load 66 N & 63 N, 20 Hz to 110 Hz) for increasing pressure ratios (P_r)

Pressure ratio*	Hybrid Brush Seal			
	$P_r = 1.0$	$P_r = 1.7$	$P_r = 2.4$	$P_r = 3.0$
Stiffness [kN/m]	93 (± 5)	130 (± 6)	141 (± 7)	141 (± 7)
Dry Friction coef., μ	0.66	0.51	0.64	0.69
Loss Factor coef., γ	0.42	0.40	0.27	0.22

*: atmospheric discharge pressure

CONCLUSIONS

This paper presents results from test to quantify the seal leakage and static and dynamic behavior at increasing pressure differentials. Flow rate (leakage) measurements demonstrate a better sealing performance of the HBS with respect to a 1st generation shoed-brush seal (SBS).

Single frequency dynamic load tests (without shaft rotation) allow identifying equivalent viscous damping coefficients as a function of the pressure differential across the seal and under non-rotating conditions. Mechanical energy dissipation parameters are identified for increasing supply pressures. The dry friction coefficient (μ) increases slightly as the pressure differential across the seal increases (5 % from $P_r = 1.0$ to $P_r = 3$). The increase of the dry friction coefficient is directly related to the increase of the contact forces between the seal components induced by the pressure differential across the seal. The loss factor coefficient (γ) (material

hysteresis) decays as the pressure ratio increases. This behavior is attributed to the repositioning of the bristles and the stiffening effect due to the pressure differential across the seal (i.e. blowdown effect).

ACKNOWLEDGEMENTS

Thanks to Siemens Power Generation Inc. for supporting the work and to Mr. John Justak, Advanced Technology Group Inc. (<http://www.advancedtg.com>), for providing the test seal.

REFERENCES

- (1) Xi J. and Rhode D. L. (2006), "Rotordynamics of Impeller Eye Seals with Wear-Damaged Teeth in Centrifugal Compressors," *Tribol. Trans*, **49**,3, pp. 328-337.
- (2) Benkert H. and Wachter J. (1980), "Flow Induced Spring Coefficients of Labyrinth Seals for Applications in Tubomachinery," NASA CP2133.
- (3) Childs D.W. and Vance J.M. (1997), "Annular Gas Seals and Rotordynamics of Compressors and Turbines," *Proc. 26th Turbomachinery Symposium*, pp.201-219.
- (4) Ferguson J.G. (1988), "Brushes as High Performance Gas Turbine Seals," ASME Paper No. 88-GT-182.
- (5) Proctor M.E. and Delgado I.R. (2004), "Leakage and Power Loss Tests Results for Competing Turbine Engine Seals," NASA TM-2004-213049.
- (6) Chupp R.E. and Dowler C.A. (1993), "Performance Characteristics of Brush Seals for Limited Life Engines," *Trans. of the ASME*, **115**, pp.390-396.
- (7) Conner J.K. and Childs D. (1993), "Rotordynamic Coefficient Test Results for a Four-Stage Brush Seal," *AIAA J. Prop. Power*, **9**, pp.113-119.
- (8) Dogu Y. and Aksit M.F. (2005), "Brush Seal Temperature Distribution Analysis," ASME Paper No. GT2005-69120.
- (9) Justak, J.F. (2002), "Robust Hydrodynamic Brush Seal," U.S. Patent No. 6,428,009.
- (10) Delgado A. San Andrés L. and Justak J.F. (2004), "Analysis of Performance and Rotordynamic Force Coefficients of Brush Seals with Reverse Rotation Ability," ASME Paper No. GT2004-53614.
- (11) Delgado A. and San Andrés L. (2005), "Measurements of Leakage, Structural Stiffness and Energy Dissipation Parameters in a Shoed Brush Seal," *Sealing Technology*, **12**, pp. 7-10.
- (12) Justak J.F. (2002), "Robust Hydrodynamic Brush Seal," U.S. Patent No. 6,428,009.
- (13) Justak J.F. and Crudginton P.F. (2006), "Evaluation of a film riding hybrid seal," AIAA Paper No. 2006-4932.